The Ups and Downs of AD Leo

Manuel Güdel & Marc Audard

Paul Scherrer Institut, Würenlingen & Villigen, CH-5232 Villigen PSI, Switzerland

Edward F. Guinan

Villanova University, Villanova, PA 19085, USA

Rolf Mewe

SRON Laboratory for Space Research, 3584 CA Utrecht, Netherlands

Jeremy J. Drake

Harvard-Smithsonian Center for Astrophysics, Cambridge, MA, 02138, USA

Ilya Y. Alekseev

Crimean Astrophysical Observatory, Nauchny, Crimea 334413, Ukraine

Abstract. We present first results of a long coordinated campaign on AD Leo, using EUVE, BeppoSAX, the VLA, and optical telescopes. The campaign comprises a time span of 44 days during which AD Leo was almost continuously the prime target of the EUVE satellite. The coronal emission was in a state of ongoing variability, raising interesting questions on the role of flare-like events for coronal heating. We discuss phenomenological signatures in the light curves and present preliminary results from BeppoSAX spectroscopy.

1. Introduction

Coronal/chromospheric flares may play an important role in the overal heating of solar/stellar coronae. In particular, the large number of small flares ("microflares", "nanoflares", e.g., Parker 1988), may well be able to heat the quiescent (i.e., quasi-steady) coronae of the Sun and stars. Solar observations show that the flare occurrence rate is distributed in energy as a power-law, $\mathrm{d}N/\mathrm{d}E \propto E^{-\alpha}$ (e.g., Lin et al. 1984). For stellar obsevations, see Audard et al. (2000). The value of α determines the importance of the low- or high-energetic tail of the distribution for coronal heating.

Flares are also pivotal in lifting chromospheric material into the corona (Antonucci et al. 1984). The flare process itself offers a multitude of interesting mechanisms for study, including particle acceleration, heating, and hydrodynamic effects (heat fronts, loop filling, pressure buildup, etc). Here, we are studying the "long-term" and statistical behavior of flare energy releases on the particularly active flare star AD Leo. We present preliminary results from a first analysis. A comprehensive report will be given elsewhere.

2. Observations

An extremely long EUVE observation was approved during EUVE's cycle 7 between April 2 and May 16, 1999 comprising (with a few minor time gaps) 900 ks of on-source exposure time. The DS instrument and the three spectrometers (SW, MW, LW) were used.

Between May 1 and May 15, we obtained a total of 270 ks of exposure time with BeppoSAX, covering about 8 days within this interval. We obtained data from the LECS (0.1–10 keV), the MECS (2–10 keV), and the PDS (15–400 keV) instruments.

On April 29, a 10 hr integration was carried out with the NRAO VLA. We used the 2 cm, 3.6 cm and 6 cm bands with the array in its D configuration.

Two optical photometry observatories (Villanova University and Crimean Astrophysical Observatory) observed AD Leo in the U, B, V, R, and I bands during several nights in April and May.

3. AD Leo

AD Leo is a dM4.5e star with a rotation period of 2.7 d (Sandmann 1985; according to our [EFG] measurements, $P_{\rm rot}$ appears to be 1.7 d only. The EUVE data will be used to search for a period).

We selected AD Leo for this campaign as it i) shows frequent optical flares; ii) many of the flares are typically sufficiently energetic and sufficiently long so as to be detectable despite the Earth blocks of the satellite (orbit period approx. 96 minutes). iii) AD Leo shows an interesting quiescent count rate in the DS spectrometer: high enough for a good detection and a clean definition of the 'background', but low enough to keep the Poisson errors sufficiently low to detect small flares. iv) Well-known optical behavior with easy flare detections in the optical U band.

4. Observational Results

An overview of the observations obtained by SAX (LECS, MECS), EUVE, the NRAO VLA, and by the two optical photometers is shown in Figure 1.

The EUVE light curve is extremely variable. Most of the fluctuations visible in Fig. 1 are real (the error bars being smaller than the dots).

A detailed comparison between the EUVE and the BeppoSAX light curves is presented in Figure 2. Note that EUV flares tend to be smoother, while continuous variability is more obvious than in the soft X-ray range. There are interesting flare examples in the EUVE light curve with gradual rise phases but very rapid decays.

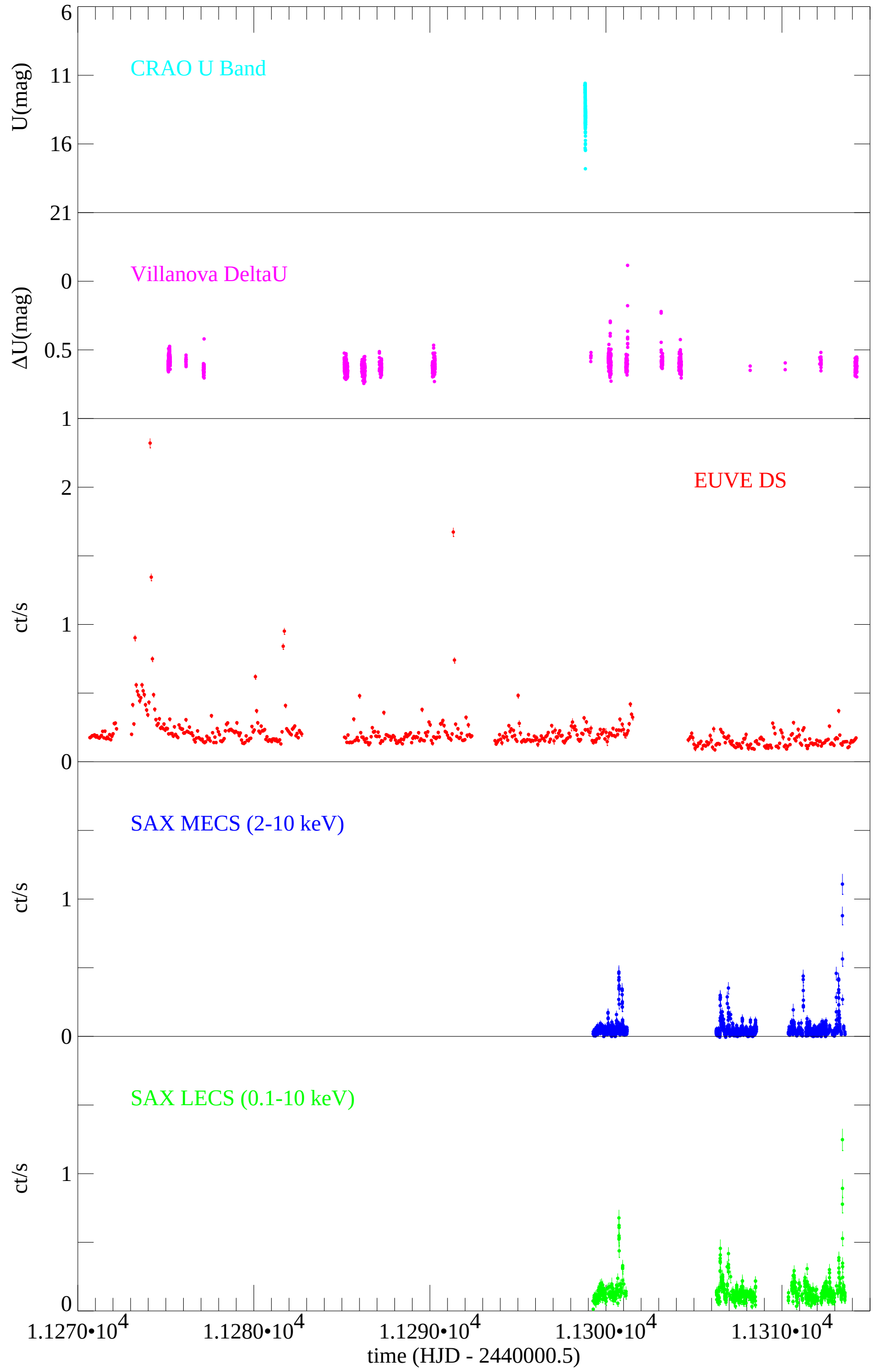

Figure 1. Overview: lightcurves from optical photometry (CRAO, Villanova), EUVE DS, SAX MECS, and SAX LECS. Note that most of the visible fluctuations in the DS curve are real (error bars $<$ dots)

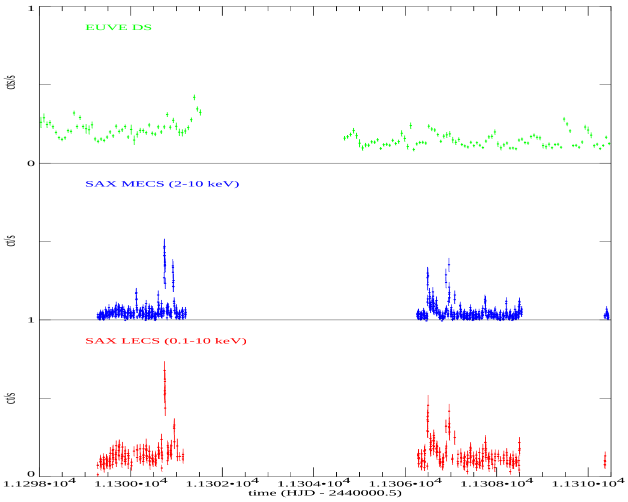

Figure 2. Example of simultaneous flaring behavior in EUV (top), 2-10 keV soft X-rays (MECS, middle), and 0.1–10 keV soft X-rays (LECS, bottom).

Figure 3a shows the large EUV flare early in this campaign. It consists of a gradual component and at least three more rapid bursts, with count rates up to 2.7 cts s^{-1}. Note the long decay over 2–3 full days.

Figure 3b correlates an exceptional optical U band flare observed at CRAO, and a weakly polarized radio flare (seen at X and U band) with the EUVE light curve. Although the optical and radio events coincide with EUVE flares, the precise relative timing is unexpected (optical/radio flares during EUVE maximum).

We show in Figure 4 the MECS light curve, and in Figure 5 the LECS and MECS spectra (all photons). Table 1 provides best-fit results of a spectral analysis with all elements except Fe kept at their solar photospheric values. One

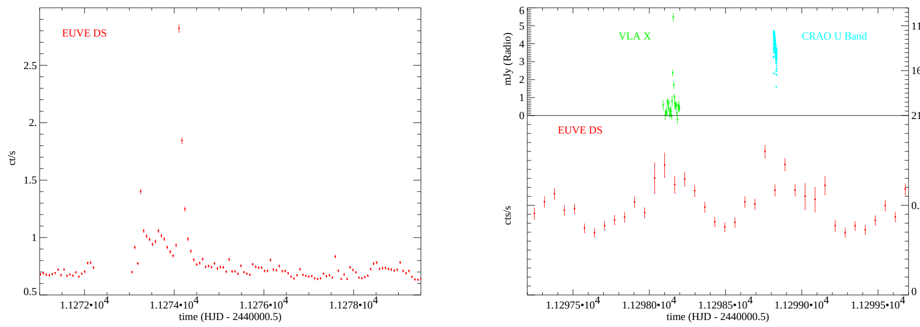

Figure 3. (a, left) Large flare complex early in the campaign. Note long decay times. (b, right) Timing between an optical U band flare observed at CRAO, a VLA radio flare, and the EUVE DS light curve.

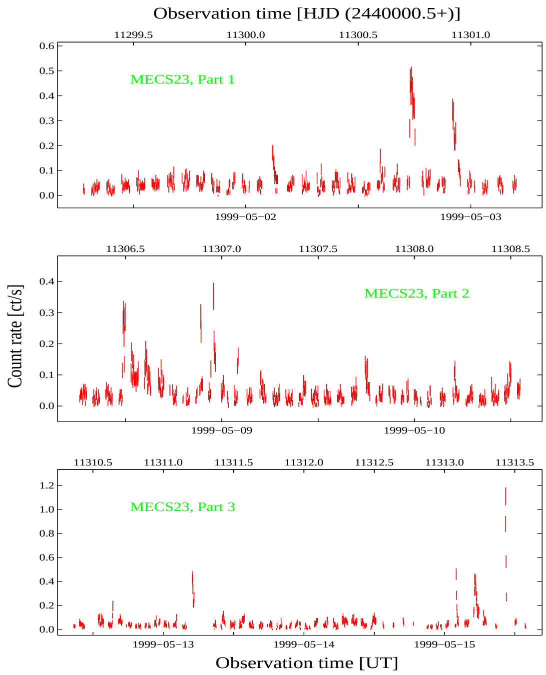

Figure 4. MECS light curve

fit uses the hydrogen column density N_{H} as a free parameter, while for the other fit we fixed N_{H} at a value compatible with AD Leo's distance. The Fe abundance converges to a rather low value of 0.5.

5. Outlook

This data set provides unique opportunities to study the statistical behavior of flares, modulations due to evolving magnetic structures, and rotational modulation on time scales more than an order of magnitude larger than the rotation period. Detailed analysis and modeling will be presented in a forthcoming paper.

Acknowledgements: We thank the CEA/EUVE, VLA, and BeppoSAX staff for their efforts to coordinate these observations. The National Radio Astronomy Observatory is a facility of the US National Science Foundation, operated under cooperative agreement by Associated Universities, Inc.

References

Audard, M., Güdel, M., Drake, J. J., & Kashyap, V., & Guinan, E. F. 2000, these proceedings

Table 1. Mekal Fits to the LECS+MECS mean spectrum

Parameter	N_H free		N_H fixed	
$\log N_H$ (cm^{-2})	19.63	(19.44, 19.73)	18.0	($\cdots$, $\cdots$)
kT_1 (keV)	0.16	(0.15 , 0.17)	0.18	(0.17 , 0.19)
$\log EM_1$ (cm^{-3})	50.87	(50.82, 50.92)	50.75	(50.71, 50.80)
kT_2 (keV)	0.69	(0.68 , 0.70)	0.70	(0.68 , 0.73)
$\log EM_2$ (cm^{-3})	51.20	(51.19, 51.21)	51.23	(51.20, 51.26)
kT_3 (keV)	2.01	(1.94 , 2.05)	2.12	(1.96 , 2.25)
$\log EM_3$ (cm^{-3})	50.97	(50.95, 50.99)	50.93	(50.90, 50.96)
Fe	0.57	(0.56 , 0.60)	0.51	(0.46 , 0.56)
f[a]	0.71	(0.69 , 0.73)	0.72	(0.70 , 0.74)
χ^2/dof[b]	362.4/335		380.3/336	

[a]f = Cross-calibration factor LECS/MECS23

[b]dof = number of degrees of freedom

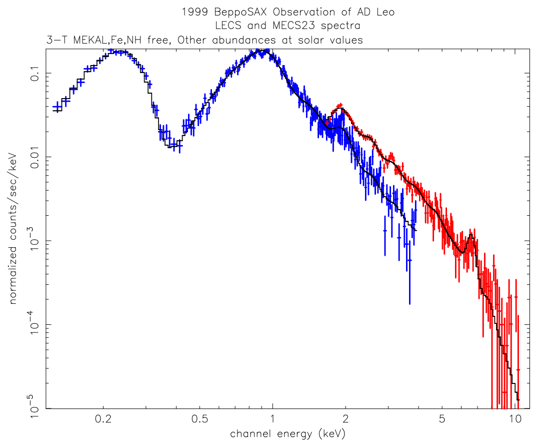

Figure 5. MECS and LECS spectra with fit.

Antonucci, E., et al. 1984, ApJ, 413, 786

Lin, R. P., Schwartz, R. A., Kane, S. R., Pelling, R. M., & Hurley, K. 1984, ApJ, 283, 421

Parker, E. N. 1988, ApJ, 330, 474

Sandmann, W. 1985, quoted in Saar, S. H., & Linsky, J. L. 1985, ApJ, 299, L47